

## The delayed basolateral membrane hyperpolarization of the bovine retinal pigment epithelium: mechanism of generation

Steven Bialek, Daniel P. Joseph and Sheldon S. Miller\*

*University of California, School of Optometry and Division of Cell and Development, Department of Molecular and Cell Biology, Berkeley, CA 94720, USA*

1. Conventional and ion-selective double-barrelled microelectrodes were used in an *in vitro* preparation of bovine retinal pigment epithelium (RPE)–choroid to measure the changes in membrane voltage, resistance and intracellular  $\text{Cl}^-$  activity ( $a_{\text{Cl}}^i$ ) produced by small, physiological changes in extracellular potassium concentration ( $[\text{K}^+]_o$ ). These apical  $[\text{K}^+]_o$  changes approximate those produced in the extracellular (subretinal) space between the photoreceptors and the RPE following transitions between light and dark.
2. Changing apical  $[\text{K}^+]_o$  from 5 to 2 mM *in vitro* elicited membrane voltage responses with three distinct phases. The first phase was generated by an apical membrane hyperpolarization, followed by a (delayed) basolateral membrane hyperpolarization (DBMH); the third phase was an apical membrane depolarization. The present experiments focus on the membrane and cellular mechanisms that generate phase 2 of the response, the DBMH.
3. The DBMH was abolished in the presence of apical bumetanide (100  $\mu\text{M}$ ); this response was completely restored after bumetanide removal.
4. Reducing apical  $[\text{K}^+]_o$ , adding apical bumetanide (500 nM), or removing apical  $\text{Cl}^-$  decreased  $a_{\text{Cl}}^i$  by  $25 \pm 6$  (n = 8),  $28 \pm 1$  (n = 2) and  $26 \pm 5$  mM (n = 3), respectively; adding 100  $\mu\text{M}$  apical bumetanide decreased  $a_{\text{Cl}}^i$  by  $12 \pm 2$  mM (n = 3). Adding apical bumetanide or removing apical bath  $\text{Cl}^-$  hyperpolarized the basolateral membrane and decreased the apparent basolateral membrane conductance ( $G_B$ ).
5. DIDS (4,4'-diisothiocyanostilbene-2,2'-disulphonic acid) blocked the RPE basolateral membrane  $\text{Cl}^-$  conductance and inhibited the DBMH and the basolateral membrane hyperpolarization produced by apical bumetanide addition or by removal of apical  $\text{Cl}^-$ . The present results show that the DBMH is caused by  $\Delta[\text{K}^+]_o$ -induced inhibition of the apical membrane  $\text{Na}^+-\text{K}^+-2\text{Cl}^-$  cotransporter; the subsequent decrease in  $a_{\text{Cl}}^i$  generated a hyperpolarization at the basolateral membrane  $\text{Cl}^-$  channel.

The chemical composition of the extracellular (subretinal) space between the neural retina and the retinal pigment epithelium (RPE) is determined by the transport activity of three cell types: Müller cells, photoreceptors and the RPE (Shimazaki & Oakley, 1984; Newman, 1985; Gallemore, Yamamoto & Steinberg, 1990; Yamamoto, Borgula & Steinberg 1992; Bialek & Miller, 1994). Light-induced changes in cell activity of the neural retina are communicated to the RPE across the subretinal space (Deary & Burnside, 1989; Joseph & Miller, 1992; Garcia & Burnside, 1994). For example, following light onset the photoreceptors generate a transient decrease in subretinal potassium concentration ( $[\text{K}^+]_o$ ) that can profoundly

affect RPE transport mechanisms at the apical and basolateral membranes (Steinberg, Linsenmeier & Griff, 1985; Joseph & Miller, 1991; Bialek & Miller, 1994). These include  $\text{K}^+$  channels, the electrogenic  $\text{Na}^+-\text{K}^+$ -ATPase, and the bumetanide sensitive  $\text{Na}^+-\text{K}^+-2\text{Cl}^-$  cotransporter (Miller & Steinberg, 1977; Oakley, Miller & Steinberg, 1978; Miller & Edelman, 1990; Edelman & Miller, 1991; Joseph & Miller, 1991; Bialek & Miller, 1994).

In the intact eye, the RPE generates several distinct components of the electroretinogram (ERG) and one of them, the ERG c-wave (Steinberg, Schmidt & Brown, 1970), is generated in part by the apical membrane  $\text{K}^+$

\*To whom correspondence should be sent at the following address: 360 Minor Hall, University of California, Berkeley, CA 94720, USA.

channels. The c-wave is followed in time by the fast oscillation (FO), which is generated by a delayed basolateral membrane hyperpolarization (Griff & Steinberg, 1984; Linsenmeier & Steinberg, 1984; Steinberg *et al.* 1985; Gallemore & Steinberg, 1993). The latter response has also been studied in the isolated RPE-choroid preparation by making changes in apical  $[K^+]_o$  from 5 to 2 mM (Griff & Steinberg, 1984; Griff, 1991; Joseph & Miller, 1991; Quinn & Miller, 1992).

In the isolated bovine RPE, decreasing apical  $[K^+]_o$  from 5 to 2 mM results in a voltage response that consists of three phases. The first corresponds to the c-wave in the intact eye which is partly generated by a diffusion potential expressed across the apical membrane  $K^+$  conductance. The second phase is the delayed basolateral membrane hyperpolarization that corresponds to the FO in the intact eye (Steinberg *et al.* 1985; Gallemore & Steinberg, 1993). Intracellular  $Cl^-$  activity ( $a_{Cl}^i$ ) decreased by 20–30 mM during phases 1 and 2 and it has been postulated that this decrease generates a hyperpolarizing diffusion potential across the basolateral membrane  $Cl^-$  conductance (Joseph & Miller, 1991). Part of this hyperpolarization could have occurred because the  $a_{Cl}^i$  decrease also decreased  $Cl^-$  conductance ( $g_{Cl}$ ) at the basolateral membrane.

The present study focuses on the *second phase* of the apical 5 to 2 mM  $K^+$  response, the so-called delayed basolateral membrane hyperpolarization (DBMH). The results demonstrate that the  $Cl^-$  transport pathway, which consists of an apical membrane bumetanide-sensitive  $Na^+-K^+-2Cl^-$  cotransporter and a basolateral membrane  $Cl^-$  conductance, is mainly responsible for generating the delayed basolateral membrane hyperpolarization and presumably the FO.

## METHODS

The bovine eyes used in our experiments were obtained commercially from a nearby slaughterhouse (Ranch Veal Corp., Petaluma, CA, USA) 15–40 min after death, placed in cold Ringer solution, and transported to the laboratory. The techniques for preparing and handling the bovine RPE-choroid, along with the recording and perfusion system have been previously described (Joseph & Miller, 1991).

The control Ringer solution contained (mM): 120 NaCl, 23  $NaHCO_3$ , 10 glucose, 5 KCl, 1.8  $CaCl_2$  and 1  $MgCl_2$ . The osmolarity of this solution was  $295 \pm 4$  mosmol  $l^{-1}$ . The Ringer solution was maintained at a temperature of  $37 \pm 1.0$  °C using Peltier heat pumps located at the apical and basal entrance ports of the perfusion chamber. In experiments where  $[K^+]_o$  was changed to 2 mM, NaCl was substituted on an equimolar basis for KCl. When  $Cl^-$  was removed from the bathing solution, NaCl was replaced with  $NaCH_3SO_4$ ;  $CaCl_2$  was replaced with  $CaSO_4$ ; and  $MgCl_2$  was replaced with  $MgSO_4$ . Since the osmolarities of the low- $Cl^-$  solutions were 20 mosmol  $l^{-1}$  higher than the control solutions, 20 mM mannitol was added to all other control solutions in the  $Cl^-$  removal experiments to prevent possible osmotic effects. Nominally  $HCO_3^-$ -free Ringer solutions were

made by substituting 10 mM Hepes buffer and 13 mM NaCl for  $NaHCO_3$ . The presence of glutathione (1 mM) in both apical and basal perfusion solutions significantly increased the longevity of the RPE explant preparation as measured by the maintenance of several membrane transport, voltage and resistance parameters (Miller & Edelman, 1990; Joseph & Miller, 1991).

Solutions containing  $HCO_3^-$  were equilibrated with 5%  $CO_2$ –10%  $O_2$ –85%  $N_2$ . The bicarbonate-free Ringer solutions were equilibrated with air. All solutions were titrated to a final pH value of  $7.5 \pm 0.1$  with NaOH or HCl if necessary. DIDS (4,4'-diisothiocyanostilbene-2,2-disulphonic acid) was obtained from Sigma Chemical Co. Solutions with DIDS were made up fresh for each experiment and protected from the light. Bumetanide was a gift from Hoffmann-LaRoche Inc., Nutley, NJ, USA. Barium was obtained from Sigma in the form  $BaCl_2$ .

### Membrane voltage and conductance measurements

The intracellular recording system and the techniques for fabricating and calibrating the  $Cl^-$ -selective double-barrelled microelectrodes have been previously described (Joseph & Miller, 1991). Briefly, calomel electrodes in series with Ringer solution-agar bridges were used to measure the transepithelial potential (TEP). The signals from intracellular microelectrodes were referenced to either the apical or basal calomel electrodes to measure the membrane potentials,  $V_A$  and  $V_B$ , where  $TEP = V_B - V_A$ . The transepithelial resistance,  $R_t$ , and the apparent ratio of the apical to basolateral membrane resistance,  $a$ , were obtained by passing 4  $\mu A$  current pulses across the tissue and measuring the resulting changes in TEP and membrane potential. Current pulses were bipolar, with a period of 3 s applied at 30 s intervals.  $R_t$  is the resulting voltage change in the TEP divided by 4  $\mu A$ , and  $a$  is the ratio of voltage change in  $V_A$  divided by the change in  $V_B$  ( $a = \Delta V_A / \Delta V_B$ ).

### Intracellular $Cl^-$ activity measurements

$Cl^-$ -selective double-barrelled microelectrodes were made using thick septum theta glass from WPI (New Haven, CT, USA). The ion-sensing barrel was silanized and filled with an ion-exchange resin (Corning 477913-Cl; CIBA Corning Diagnostics, Norwood, MA, USA), then back-filled with 150 mM KCl; the reference barrel was filled with 150 mM lithium acetate plus 1 mM KCl. The resistance of the ion-sensing barrel was 20–60 G $\Omega$  and the reference barrel resistance was 125–175 M $\Omega$ . The time constant for the ion-sensing barrels was 6–12 s.

The electrodes were calibrated before and after each experiment using the following solutions: 10 mM KCl, 25 mM KCl, 100 mM KCl, control Ringer solution and 100 mM  $KHCO_3$ . The electrode slope was determined from the voltage responses in 10, 25 and 100 mM KCl. These responses are a linear function of the log  $Cl^-$  activity between 10 and 100 mM KCl; the slope of the calibration curve for each microelectrode was determined by linear regression analysis. Electrode selectivity was calculated from the voltage responses in 100 mM KCl and 100 mM  $KHCO_3$ . The calibration curves had a mean slope of  $53.7 \pm 2.4$  mV; the selectivity for  $HCO_3^-$  over  $Cl^-$  was  $0.11 \pm 0.04$  (mean  $\pm$  s.d.,  $n = 54$  electrodes).

The acceptance criterion for the  $Cl^-$ -selective double-barrelled microelectrodes was as follows: for the reference barrel, the measured potential difference between the control Ringer solution and the 100 mM KCl solution had to be less than 5 mV. For the  $Cl^-$ -sensing barrel, the  $HCO_3^-$ - $Cl^-$  selectivity had to be less than 0.16, and the slope measured during the calibration had

to fall between 51 and 60 mV. Intracellular  $\text{Cl}^-$  activity was calculated using the Nicolsky equation (Garcia-Diaz, 1984):

$$a_{\text{Cl}^-}^i = (a_{\text{Cl}^-}^o + S_{\text{HCO}_3^-/\text{Cl}^-} \times a_{\text{HCO}_3^-}^o) \times 10^{(V_{\text{Cl}^-}/M)}, \quad (1)$$

where  $S_{\text{HCO}_3^-/\text{Cl}^-}$  is the selectivity of the electrode for  $\text{HCO}_3^-$  over  $\text{Cl}^-$  measured during the calibration,  $a_{\text{Cl}^-}^o$  and  $a_{\text{HCO}_3^-}^o$  are the  $\text{Cl}^-$  and  $\text{HCO}_3^-$  activities in the extracellular bathing solution (99 and 18 mM, respectively, for control Ringer solution),  $V_{\text{Cl}^-}$  is the difference in the voltages measured by the  $\text{Cl}^-$ -sensing barrel and the reference barrel, and  $M$  is the slope of the electrode measured during the calibration. The activity coefficient for  $\text{Cl}^-$  and  $\text{HCO}_3^-$  was assumed to be 0.76 (Weast, 1978). The single- and double-barrelled electrodes (reference barrel) were used to measure membrane voltages and resistance ratios. No statistically significant difference was found between the measurements from either type of recording electrode.

### pH<sub>i</sub> measurements

Intracellular pH (pH<sub>i</sub>) was measured using the pH-sensitive dye 2',7'-bis(carboxyethyl)-5(6)-carboxyfluorescein (BCECF) (Rink, Tsien & Pozzan, 1982) in a ratioing fluorimetry technique. The excitation light source was a 75 W xenon lamp (Ushio Inc., Shiba, Tokyo). The excitation wavelength was switched every half second between 440 and 480 nm using interference filters with a 10 nm bandwidth (Omega Optical, Inc., Brattleboro, VT, USA), and the epifluorescent emission was measured through a 40 nm bandwidth filter at 520–560 nm using a photomultiplier tube (Thorn EMI, Ruislip, Middlesex, UK). The voltage and fluorescence signals were digitized and stored on an IBM-compatible 386 computer for later analysis.

As previously described (Lin & Miller, 1991, 1994; Kenyon, Yu, La Cour & Miller, 1994) background fluorescence was measured at each excitation wavelength after mounting an RPE-choroid explant in a modified Ussing chamber. This procedure was carried out before loading the RPE with BCECF. After completion of an experiment, a four-point calibration between pH 6.8 and 8.0 was performed using the method of Thomas *et al.* (1979). Calibration solutions contained (mM): 80 KCl, 10 *N*-2-hydroxyethylpiperazine-*N'*-2-ethanesulphonic acid (Hepes), 10 2-*N*-morpholinoethanesulphonic acid (MES), 1 MgCl<sub>2</sub>, 1.8 CaCl<sub>2</sub>, 10 D-glucose, and 95 mannitol. Nigericin (2 mM), a  $\text{K}^+$ - $\text{H}^+$  exchanger, was added to the apical bath to ensure equilibration of pH<sub>i</sub> and pH<sub>o</sub> (by matching  $[\text{K}^+]_i$  and  $[\text{K}^+]_o$ ). All chemicals were obtained from Sigma Chemical Co.

### Equivalent circuit

The RPE cells can be modelled as an equivalent electrical circuit (Miller & Steinberg, 1977). The apical and basolateral membranes are modelled as electromotive forces,  $E_A$  and  $E_B$ , respectively, in series with resistors,  $R_A$  and  $R_B$ .  $R_S$  is the paracellular resistive pathway composed of the junctional complexes between the cells, and the damaged cells around the edge of the tissue which is mechanically sealed between two Lucite plates. As a result of the difference in voltage between  $E_A$  and  $E_B$  a current ( $I_S$ ) flows around the circuit and:

$$V_A = E_A - I_S R_A, \quad (2)$$

$$V_B = E_B - I_S R_B. \quad (3)$$

The apical and basolateral membrane voltages are electrically coupled via  $R_S$ . This means that a voltage change at one membrane will be shunted to the opposite membrane and cause a similar but smaller voltage change. In Fig. 1, for example, the phase 1 voltage response was generated by a hyperpolarization

of the apical membrane, which was passively shunted to the basolateral membrane. A membrane voltage change originating at the apical membrane ( $\Delta V_A$ ) will produce a smaller voltage change with the same time course at the basolateral membrane ( $\Delta V_B$ ) given by:

$$\Delta V_B = \Delta V_A (R_B / (R_B + R_S)), \quad (4)$$

where  $\Delta V_B$  and  $\Delta V_A$  are the observed changes in membrane voltage, and the resistances are assumed to be constant during the change (Oakley *et al.* 1978).

### Determination of $G_B$ and $E_B$

A conclusion of this study is that the  $[\text{K}^+]_o$ -induced decrease in  $a_{\text{Cl}^-}^i$  hyperpolarized the basolateral membrane, either by altering the  $\text{Cl}^-$  equilibrium potential ( $E_{\text{Cl}^-}$ ) or by a  $\Delta a_{\text{Cl}^-}^i$ -induced change in the basolateral membrane conductance ( $G_B$ ). Since the bovine RPE basolateral membrane is predominantly conductive to  $\text{Cl}^-$  and  $\text{K}^+$  (Joseph & Miller, 1991; Bialek & Miller, 1994), the basolateral membrane battery ( $E_B$ ) can be written as:

$$E_B \approx T_{\text{Cl}^-}^B E_{\text{Cl}^-} + T_{\text{K}^+}^B E_{\text{K}^+}, \quad (5)$$

where  $T_{\text{Cl}^-}^B = g_{\text{Cl}^-}^B / G_B$  and  $T_{\text{K}^+}^B = g_{\text{K}^+}^B / G_B$ ; they are the relative  $\text{Cl}^-$  and  $\text{K}^+$  conductances of the basolateral membrane and  $G_B$  is the total basolateral membrane conductance ( $G_B = g_{\text{Cl}^-}^B + g_{\text{K}^+}^B$ ).  $E_{\text{Cl}^-}$  and  $E_{\text{K}^+}$ , the Nernst potentials for  $\text{Cl}^-$  and  $\text{K}^+$ , were calculated using the bulk solution values for  $[\text{K}^+]_o$  and  $[\text{Cl}^-]_o$ . These values differ slightly from the subchoroidal concentrations just adjacent to the basolateral membrane.  $[\text{K}^+]_o$  was measured as  $6.1 \pm 0.5$  mM ( $n = 3$ ) in the subchoroidal space (Bialek & Miller, 1994); this would alter the calculated  $E_{\text{K}^+}$  by as much as 5 mV and would at most cause a 6% error.  $[\text{Cl}^-]_o$  in the subchoroidal space was also found to be slightly higher (1–2 mM) than in the bulk solution, but because  $[\text{Cl}^-]_o$  is high (approximately 130 mM) the error in the calculated  $E_{\text{Cl}^-}$  is negligible (less than 0.5 mV). These errors are too small to effect any of our conclusions.

Assuming that the basolateral membrane is only conductive to  $\text{Cl}^-$  and  $\text{K}^+$ , eqn (5) can be rewritten as:

$$T_{\text{Cl}^-}^B = (E_B - E_{\text{K}^+}) / (E_{\text{Cl}^-} - E_{\text{K}^+}), \quad (6)$$

From the RPE equivalent circuit (Miller & Steinberg, 1977),  $\text{TEP} = I_S R_S$ . Substitution for  $I_S$  in eqn (3) gives  $E_B$  in terms of basolateral membrane voltage and resistance:

$$E_B = V_B - \text{TEP} (R_B / R_S), \quad (7)$$

where

$$R_B = \frac{1}{G_B} = \left( \frac{1}{1 + a} \right) \left( \frac{R_S R_t}{R_S - R_t} \right), \quad (8)$$

and  $R_S$  is assumed to be  $1.14 R_t$  (Joseph & Miller, 1991). The present data was used in eqns (6)–(8) to calculate the time course of the changes in  $T_{\text{Cl}^-}^B$  (and  $T_{\text{K}^+}^B$ ) during the apical change in  $[\text{K}^+]_o$  from 5 to 2 mM.

### Isolated $V_B$

The RPE response to a step decrease of apical  $[\text{K}^+]_o$  has several overlapping components (see Fig. 1). One of these components is a delayed hyperpolarization of  $V_B$  measured during phase 2 (Linsenmeier & Steinberg, 1984; Joseph & Miller, 1991). Since  $V_A$  and  $V_B$  are electrically coupled, part of this hyperpolarization originated at the apical membrane because of the  $[\text{K}^+]_o$ -induced increase in  $E_{\text{K}^+}$ . The voltage generated solely at the basolateral membrane during phase 2 was estimated by subtracting the observed basolateral membrane potential ( $V_B$ ) and the voltage contribution passively shunted from the apical membrane. The fraction of voltage shunted from the apical membrane,

$V_A(\Delta V_B/\Delta V_A)$ , was estimated by measuring  $\Delta V_B/\Delta V_A$  during the first 10 s of the low  $K^+$  response, when there was little or no contribution from the basolateral membrane (eqn (4)). This ratio was used at subsequent points in time to calculate the isolated basolateral membrane hyperpolarization:  $(V_B - V_A)(\Delta V_B/\Delta V_A)$ .

### Statistical analysis

Statistical data are given as means  $\pm$  s.d. When appropriate, significance was determined using Student's *t* test.

## RESULTS

Figure 1 shows that a step decrease of apical  $[K^+]_o$  from 5 to 2 mM produced a voltage response with three operationally distinct phases, indicated by the vertical lines. The record at the top of the figure shows the  $\Delta[K^+]_o$ -induced changes in TEP and  $R_t$ ; the changes in  $V_A$ ,  $V_B$  and  $a$  ( $R_A/R_B$ ) are shown in the middle of the figure;  $a_{Cl}^i$  is shown in the lower trace. During phase 1, the apical membrane hyperpolarized at a faster rate than the basolateral membrane and therefore the TEP increased. By the end of phase 1, the apical membrane had hyperpolarized by  $\sim 12$  mV, TEP increased by 1.0 mV, and  $a_{Cl}^i$  decreased by 8 mM;  $a$  decreased from 0.21 to 0.12 and  $R_t$  decreased slightly.

By definition, the start of phase 2 occurred when the TEP reversed direction and began to decrease. Since  $V_A$  and  $V_B$  continued to hyperpolarize there must have been an extra, 'delayed' hyperpolarization generated at the basolateral membrane. During this second phase  $V_B$  hyper-

polarized by 10.2 mV, TEP decreased by 2.1 mV, and  $a_{Cl}^i$  decreased by 10 mM;  $a$  decreased from 0.12 to 0.10 and  $R_t$  increased from 125 to 133  $\Omega$  cm<sup>2</sup>.

In phase 3, the rate of apical membrane depolarization exceeded the rate of basolateral membrane depolarization and the TEP decreased. These voltage changes are probably generated by an inhibition of the apical membrane  $Na^+-K^+$  pump, a change in apical  $E_K$ , or a decrease in apical membrane  $K^+$  conductance (Joseph & Miller, 1991; Bialek & Miller, 1994); these phase 3 responses are generally small and will not be discussed further. The membrane voltages and resistances as well as the  $a_{Cl}^i$  always returned to baseline following the elevation of apical  $[K^+]_o$  back to 5 mM.

The results summarized in Fig. 1 were corroborated in a series of similar experiments. In control Ringer solution (5 mM  $K_o^+$ ), intracellular  $Cl^-$  activity was  $64.5 \pm 1.8$  mM (mean  $\pm$  s.d.;  $n = 28$ ). Phase 1 occurred following the transition from 5 to 2 mM  $K_o^+$  and lasted for 30 to 60 s. The apical membrane hyperpolarized by  $14.0 \pm 0.6$  mV, the TEP increased  $0.8 \pm 0.1$  mV ( $n = 25$ ) and  $a_{Cl}^i$  decreased by  $6.0 \pm 0.8$  mM ( $n = 8$ );  $a$  decreased by  $24 \pm 12\%$  and there was no statistically significant change in  $R_t$  ( $n = 6$ ). During phase 2, which generally lasted for 1–2 min, the basolateral membrane hyperpolarized by  $6.4 \pm 0.7$  mV and the TEP decreased  $1.3 \pm 0.2$  mV ( $n = 25$ );  $a_{Cl}^i$  decreased by  $14 \pm 1.5$  mM ( $n = 8$ ). During this time there

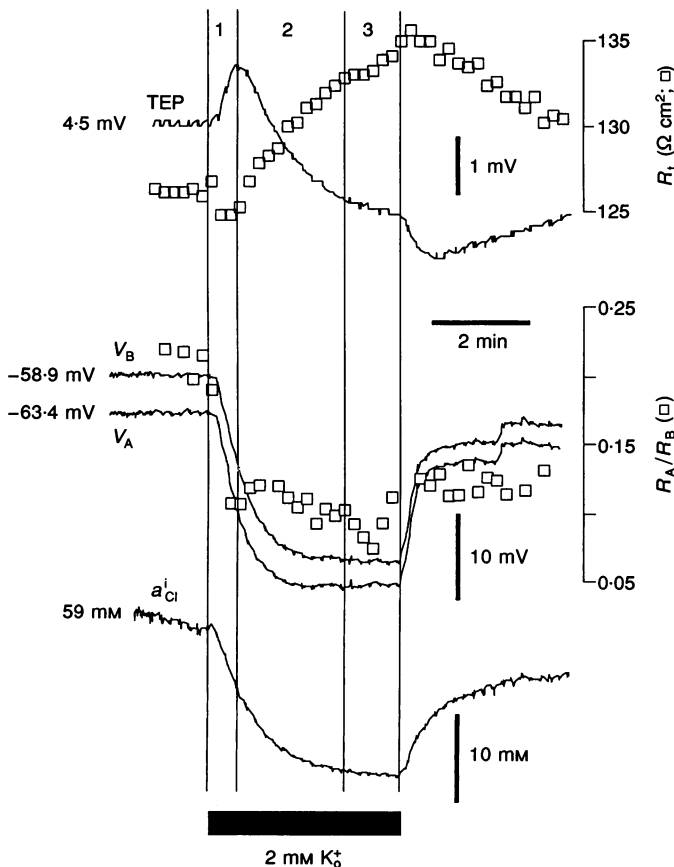


**Figure 1. The apical 5 to 2 mM  $K_o^+$  response has three phases**

The effect of changing apical bath  $[K^+]_o$  from 5 to 2 mM on TEP,  $R_t$ ,  $V_A$ ,  $V_B$ ,  $a$  ( $R_A/R_B$ ) and  $a_{Cl}^i$ . An upward deflection represents increasing positive voltage or increasing  $Cl^-$  activity. The three phases of the response delineated by the vertical lines are described in the text.

**Table 1. Isolated basal membrane response**

$\Delta[K^+]_o$ (apical)	$\Delta V_B$ (mV)			
	Control	Bumetanide	DIDS	Ba <sup>2+</sup>
5 to 0.5 mM	3.1 ± 0.7 (5)	—	—	3.5 ± 1.0 (4)
5 to 2 mM	1.9 ± 0.5 (9)	0.18 ± 0.1 (6)	0.3 ± 0.2 (4)	1.1 ± 0.3 (2)

In these experiments either 0.1 mM bumetanide was added to the apical bathing solution, or 5 mM Ba<sup>2+</sup> or 3 mM DIDS was added to the basal bathing solution. The values are provided as means ± s.d. and the number of cells is given in parentheses. Each experiment was performed using tissues from at least two different eyes.

was a 20 ± 4% decrease in *a* and a 10 ± 6 Ω cm<sup>2</sup> increase in *R<sub>t</sub>* (*n* = 6). These resistance changes are consistent with a decrease in basolateral membrane conductance probably caused in part by the decrease in *a*<sub>Cl<sup>-</sup></sub><sup>i</sup> (see Discussion).

**Ionic dependence of the DBMH**

The large decrease of *a*<sub>Cl<sup>-</sup></sub><sup>i</sup> in Fig. 1 suggests that the delayed basolateral membrane hyperpolarization (DBMH), which occurred during phase 2, could be generated by a change in *E*<sub>Cl<sup>-</sup></sub> or *g*<sub>Cl<sup>-</sup></sub> at the basolateral membrane. This possibility was confirmed using DIDS, which specifically blocks the RPE basolateral membrane Cl<sup>-</sup> conductance (Biagi, 1985; Miller & Edelman, 1990; Joseph & Miller, 1991; Bialek & Miller, 1994). Basal DIDS had no effect on the  $\Delta[K^+]_o$ -

induced phase 1 hyperpolarization but it abolished phase 2 and inhibited the  $\Delta[K^+]_o$ -induced *a*<sub>Cl<sup>-</sup></sub><sup>i</sup> decrease by 52 ± 22% (*n* = 4) (Bialek & Miller, 1994). The results summarized in Table 1 (column 4) show that the ‘isolated’ basolateral membrane hyperpolarization, the DBMH generated solely at the basolateral membrane (Methods), is reduced by 84% in the presence of basal DIDS.

Besides a  $\Delta a_{Cl^-}^i$ -induced change in *E*<sub>Cl<sup>-</sup></sub> or *g*<sub>Cl<sup>-</sup></sub>, we considered the possibility that a pH-sensitive basolateral membrane Cl<sup>-</sup> conductance could have contributed to the DBMH. It has been demonstrated in bovine RPE that reducing apical [K<sup>+</sup>]<sub>o</sub> from 5 to 2 mM acidified the cells by 0.30 ± 0.14 pH units (*n* = 19) (Kenyon, Miller & Adorante, 1990) and therefore pH<sub>i</sub>-dependent basolateral membrane

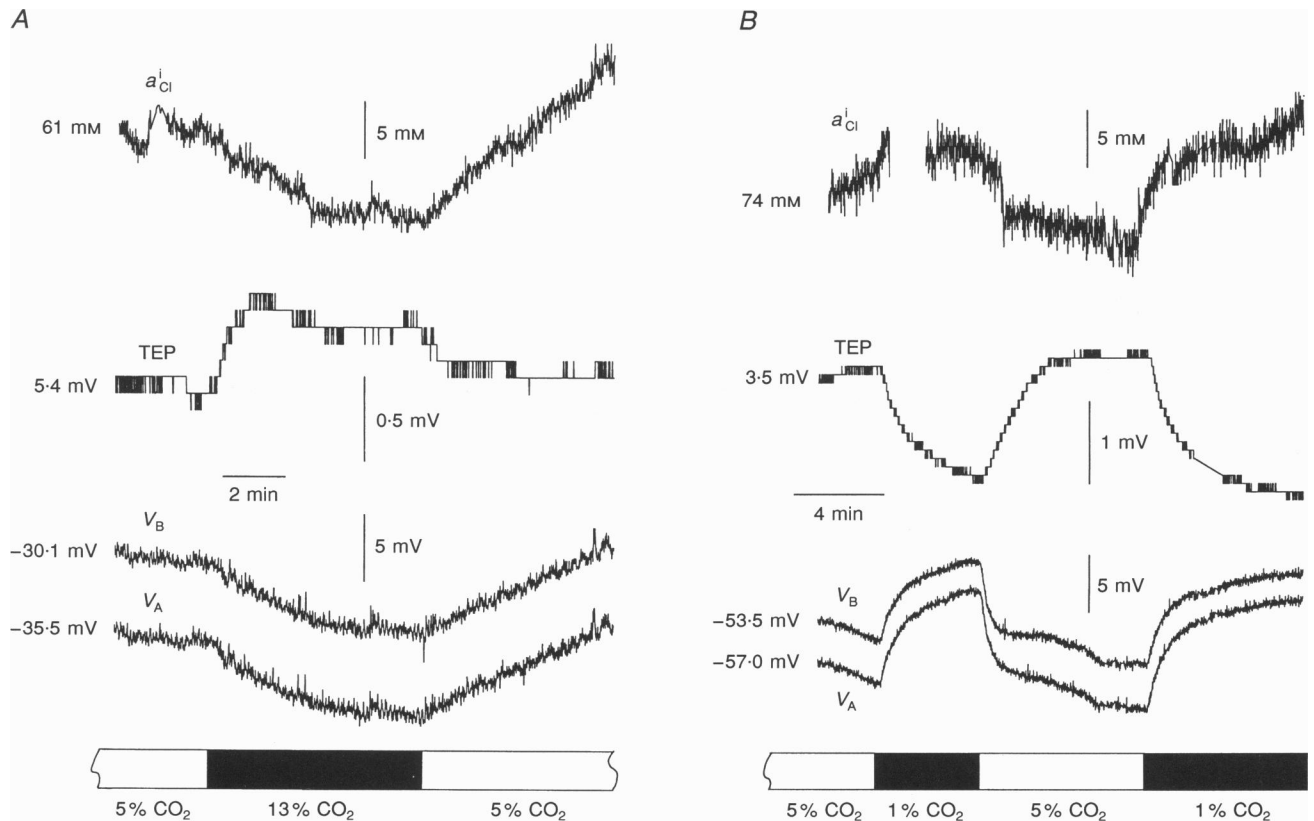


**Figure 2. Changing *P*<sub>CO<sub>2</sub></sub> (pH) alters *a*<sub>Cl<sup>-</sup></sub><sup>i</sup>**

*A*, increasing bath *P*<sub>CO<sub>2</sub></sub> from 5 to 13% decreased *a*<sub>Cl<sup>-</sup></sub><sup>i</sup>, increased TEP and hyperpolarized *V<sub>A</sub>*.  
*B*, decreasing bath *P*<sub>CO<sub>2</sub></sub> from 5 to 1% increased *a*<sub>Cl<sup>-</sup></sub><sup>i</sup>, decreased TEP and depolarized *V<sub>A</sub>*.

voltage changes or  $\text{pH}_i$  ( $[\text{HCO}_3^-]$ )-dependent changes in cell  $\text{Cl}^-$  activity could contribute to the delayed basolateral membrane hyperpolarization. This possibility was tested by changing apical and basal bath  $\text{CO}_2$  and measuring the resulting  $\text{pH}$  changes along with the changes in intracellular  $\text{Cl}^-$  activity and membrane voltage and resistance.

Fluorescence microscopy using the  $\text{pH}$ -sensitive dye BCECF was used to determine the relationship between bath  $\text{CO}_2$  and  $\text{pH}_i$ ; intracellular  $\text{pH}$  was determined at bath  $\text{CO}_2$  levels of 1, 5, 8 and 13%. The results were fitted to a line of slope 0.068  $\text{pH}$  units per unit change in percentage  $\text{CO}_2$  ( $n=5$ ). Using double-barrelled  $\text{Cl}^-$ -selective microelectrodes,  $a_{\text{Cl}}^i$  was determined when bath  $\text{CO}_2$  was 1, 5 and 13% ( $n=4$ ). These results were fitted to a line of slope  $-1.3 \text{ mM } a_{\text{Cl}}^i$  per unit change in percentage  $\text{CO}_2$ . The  $\text{pH}_i$  and  $a_{\text{Cl}}^i$  measurements at each percentage  $\text{CO}_2$  were combined to estimate the maximum possible decrease in  $a_{\text{Cl}}^i$  per unit change in  $\text{pH}_i$ . This putative  $\text{pH}_i$ -induced  $a_{\text{Cl}}^i$  decrease could only account for 16% of the observed  $\Delta[\text{K}^+]_o$ -induced change in  $a_{\text{Cl}}^i$  (Fig. 1, see Discussion).

Figure 2A and B illustrates the typical effects of changing bath  $P_{\text{CO}_2}$  on  $a_{\text{Cl}}^i$  and membrane potential. In three tissues, increasing  $\text{CO}_2$  from 5 to 13% decreased  $\text{pH}_i$  from

$7.5 \pm 0.1$  to  $7.0 \pm 0.2$  (E. Kenyon & S. S. Miller, unpublished observations) and decreased  $a_{\text{Cl}}^i$  by  $9 \pm 2 \text{ mM}$ . In these experiments, there was a  $3.3 \pm 1.4 \text{ mV}$  apical membrane hyperpolarization, sometimes followed by an apparently separate basolateral membrane depolarization of 3–5 mV. The steady-state TEP increased by  $1.8 \pm 0.9 \text{ mV}$ .  $R_t$  transiently decreased by  $2 \pm 1 \Omega \text{ cm}^2$  and then increased by  $6 \pm 2 \Omega \text{ cm}^2$  in the steady state;  $a$  decreased by  $42 \pm 12\%$ . Figure 2B illustrates the effect of decreasing  $\text{CO}_2$  from 5 to 1%, which had the opposite effect on  $a_{\text{Cl}}^i$ ,  $V_A$ ,  $R_t$  and  $a$ . In a series of these experiments,  $a_{\text{Cl}}^i$  increased by  $7 \pm 2 \text{ mM}$  ( $n=3$ ),  $\text{pH}_i$  increased by  $0.4 \pm 0.2$  ( $n=3$ ),  $V_A$  depolarized by  $7.1 \pm 2.7 \text{ mV}$  and TEP decreased by  $1.6 \pm 0.7 \text{ mV}$  ( $n=14$ );  $R_t$  increased by  $3 \pm 1.5 \Omega \text{ cm}^2$  and  $a$  increased by  $76 \pm 38\%$  ( $n=11$ ). The  $\Delta\text{CO}_2$ -induced voltage and resistance changes are consistent with a  $\text{pH}$ -sensitive electrogenic mechanism at the apical membrane with a reversal potential more negative than the resting membrane potential; this mechanism may secondarily cause  $a_{\text{Cl}}^i$  to change when  $\text{pH}_i$  changes (see Discussion).

Next we examined the effects of removing  $\text{HCO}_3^-$  from both sides of the tissue prior to the step decrease in apical  $[\text{K}^+]_o$ . Figure 3 shows that  $\text{HCO}_3^-$  removal from both

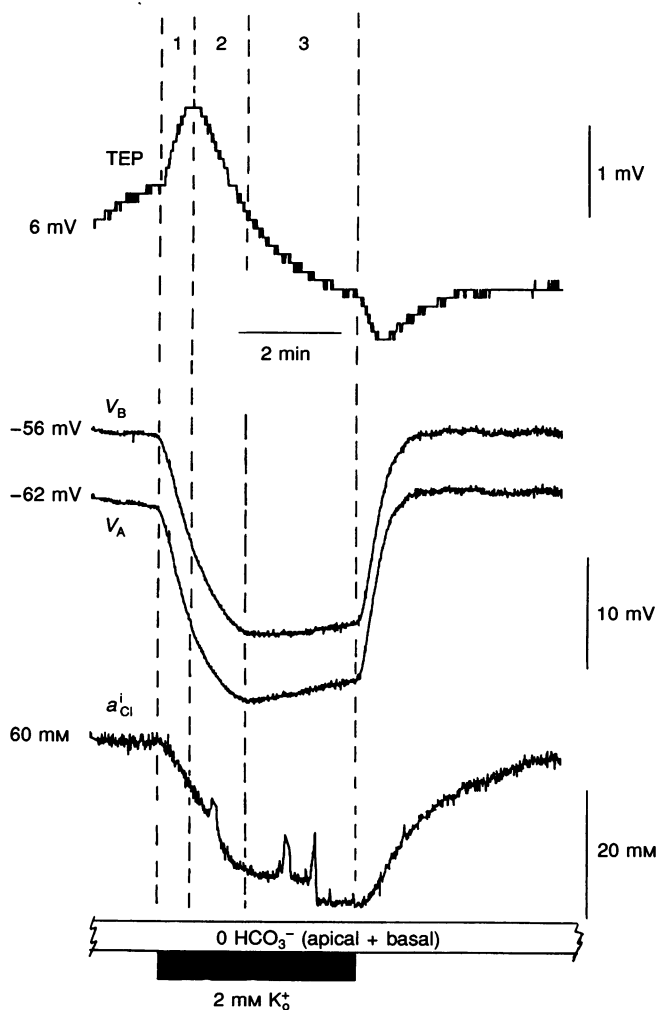


**Figure 3.  $\text{HCO}_3^-$  removal does not alter the apical 5 to 2  $\text{mM } \text{K}_o^+$  response**

The effect of  $\text{HCO}_3^-$  removal (Hepes buffered) on the apical  $[\text{K}^+]_o$  response. The dashed lines indicate the boundaries of phases 1, 2 and 3. The TEP,  $V_A$ ,  $V_B$  and  $a_{\text{Cl}}^i$  responses are very similar to those observed in the presence of  $\text{HCO}_3^-$  (see Fig. 1).

bathing solutions had no apparent effect on the delayed basolateral membrane hyperpolarization. Prior to the step decrease of apical  $[K^+]_o$  the tissue was bathed in nominally  $HCO_3^-$ -free Ringer solution for 20 min. The subsequent  $\Delta[K^+]_o$ -induced membrane potential and  $a_{Cl}^i$  changes were practically identical to control. In two additional experiments there was no effect of external  $HCO_3^-$  removal on phase 2 voltage changes, or on the decrease of  $a_{Cl}^i$ . Therefore, the basolateral membrane  $HCO_3^-$ - $Cl^-$  exchanger or other  $HCO_3^-$ -dependent mechanisms do not play a significant role in generating the DBMH.

The possible contribution of basolateral membrane  $K^+$  conductance to the delayed basolateral membrane hyperpolarization was also tested by making apical  $[K^+]_o$  changes in the presence of 5 mM basal  $Ba^{2+}$  (Joseph & Miller, 1991). The results summarized in Table 1 show

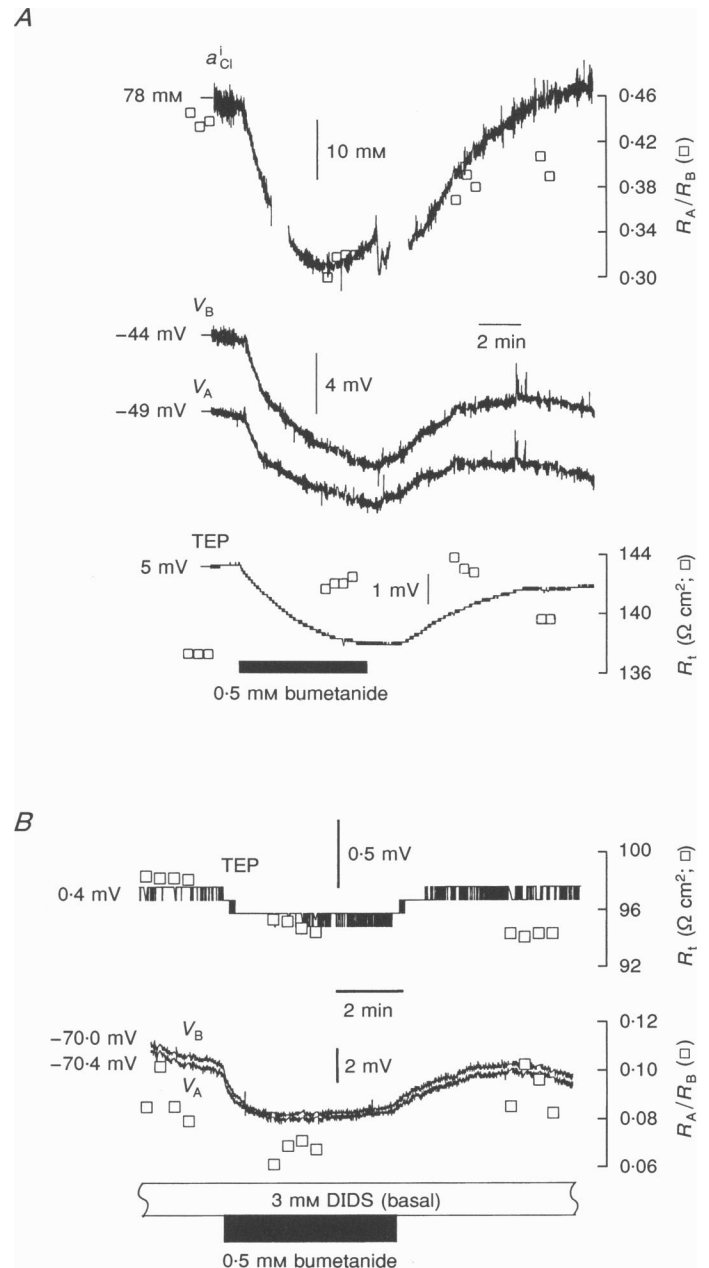
that the isolated basolateral membrane hyperpolarization caused by changing apical  $[K^+]_o$  is not significantly altered in the presence of basal  $Ba^{2+}$ . Therefore the basolateral membrane  $K^+$  conductance does not play a major role in the generation of phase 2.

**DBMH: role of the apical membrane  $Na^+-K^+-2Cl^-$  cotransporter**

In the bovine RPE reducing apical  $[K^+]_o$  caused  $K^+$  and  $Cl^-$  exit from the apical and basolateral membranes, respectively; it also decreased the inward driving force on the apical membrane  $Na^+-K^+-2Cl^-$  cotransporter (Bialek & Miller, 1994). If the DBMH resulted from a decrease in  $a_{Cl}^i$  due to inhibition of the apical membrane  $Na^+-K^+-2Cl^-$  cotransporter, then it should be possible to cause similar changes by inhibiting the cotransporter with apical bumetanide or by removing apical bath  $Cl^-$ . Figure 4A

**Figure 4. Apical bumetanide produces a  $V_B$  hyperpolarization that can be inhibited by DIDS**

*A*, the effect of adding bumetanide (0.5 mM) to the apical bath.  $a_{Cl}^i$  and apparent  $a$  follow the same time course; both decreased in response to bumetanide addition ( $a_{Cl}^i$  dropped by ~30 mM) and slowly returned to baseline after bumetanide removal (upper trace). The middle trace shows that  $V_A$  and  $V_B$  both hyperpolarized in response to bumetanide addition, but  $V_B$  hyperpolarized at a faster rate than  $V_A$ . The lower trace shows that TEP decreased and  $R_t$  increased in response to bumetanide. *B*, the effect of apical bumetanide (0.5 mM) on TEP and  $R_t$  (upper trace), and  $V_A$ ,  $V_B$  and  $a$  (lower trace) – all in the presence of basal DIDS (3 mM). Basal DIDS significantly reduced the hyperpolarization elicited by apical bumetanide and also inhibited the bumetanide-induced resistance changes.



shows that 0.5 mM apical bumetanide caused  $V_B$  to hyperpolarize by 8.6 mV (middle panel) and TEP to decrease by 2.6 mV (bottom panel). These voltage changes were accompanied by a rapid 28 mM decrease in  $a_{Cl}^i$  (top panel). During this time,  $a$  decreased from 0.45 to 0.32 and  $R_t$  increased from 137 to 143  $\Omega\text{ cm}^2$ , consistent with a conductance decrease at the basolateral membrane. An analysis using the measured changes in  $a$  and  $R_t$ , along with a range of possible  $R_s$  values, indicates that  $G_B$  significantly decreased following apical bumetanide addition (see Discussion).

Similar results were obtained in five tissues: 0.5 mM bumetanide caused  $V_B$  to hyperpolarize by  $9.7 \pm 2.1$  mV and TEP to decrease by  $1.8 \pm 0.5$  mV ( $n = 5$ );  $a$  decreased by  $35 \pm 7\%$  and  $R_t$  increased by  $5.8 \pm 1.2$   $\Omega\text{ cm}^2$  ( $n = 3$ );  $a_{Cl}^i$  decreased by  $28.5 \pm 0.5$  ( $n = 2$ ). The time course of the resistance changes coincide monotonically with the decrease in  $a_{Cl}^i$ . Similarly, apical addition of 0.1 mM bumetanide caused  $V_B$  to hyperpolarize by  $9.4 \pm 2.7$  mV, TEP to decrease by  $1.7 \pm 1.3$  mV and  $a_{Cl}^i$  to decrease by  $12 \pm 1.8$  mM ( $n = 3$ ).

If the basolateral membrane hyperpolarization seen in Fig. 4A is due to a decrease in  $a_{Cl}^i$  expressed across the  $Cl^-$  channel, then it should be inhibited by basal DIDS. In

seven tissues, basal DIDS (3 mM) hyperpolarized  $V_B$  by  $17.9 \pm 8.5$  mV ( $n = 7$ ) and increased  $a_{Cl}^i$  by  $10 \pm 5$  mM ( $n = 3$ ). Figure 4B shows the membrane voltage and resistance responses to apical bumetanide (0.5 mM) in the presence of 3 mM basal DIDS.  $V_B$  hyperpolarized by 2.9 mV and TEP decreased by 0.3 mV. In three tissues the mean  $V_B$  hyperpolarization was  $2.0 \pm 0.9$  mV and the TEP decrease was  $0.2 \pm 0.1$  mV; both  $a$  and  $R_t$  decreased slightly. Thus, basal DIDS inhibited the bumetanide-induced  $V_B$  hyperpolarization by 80% and practically abolished the bumetanide-induced changes in  $a$  and  $R_t$ .

Apical  $Cl^-$  removal should mimic the effects of bumetanide by inhibiting (or reversing) the  $Na^+-K^+-2Cl^-$  co-transporter. Figure 5A shows that when  $Cl^-$  was removed from the apical bathing solution (equimolar replacement with  $CH_3SO_4$ ) there was an initial rapid increase in TEP (upper panel) that is mainly due to a liquid junction potential at the apical voltage-sensing agar bridge. The subsequent decrease in TEP (3.4 mV) was caused by the hyperpolarization of the basolateral membrane (12.1 mV).  $R_t$  increased from 175 to 221  $\Omega\text{ cm}^2$  and  $a$  decreased from 0.18 to 0.09. These results were corroborated in a series of similar experiments in which apical  $Cl^-$  removal hyperpolarized  $V_B$  by  $14.8 \pm 1.6$  mV ( $n = 5$ ), decreased TEP by

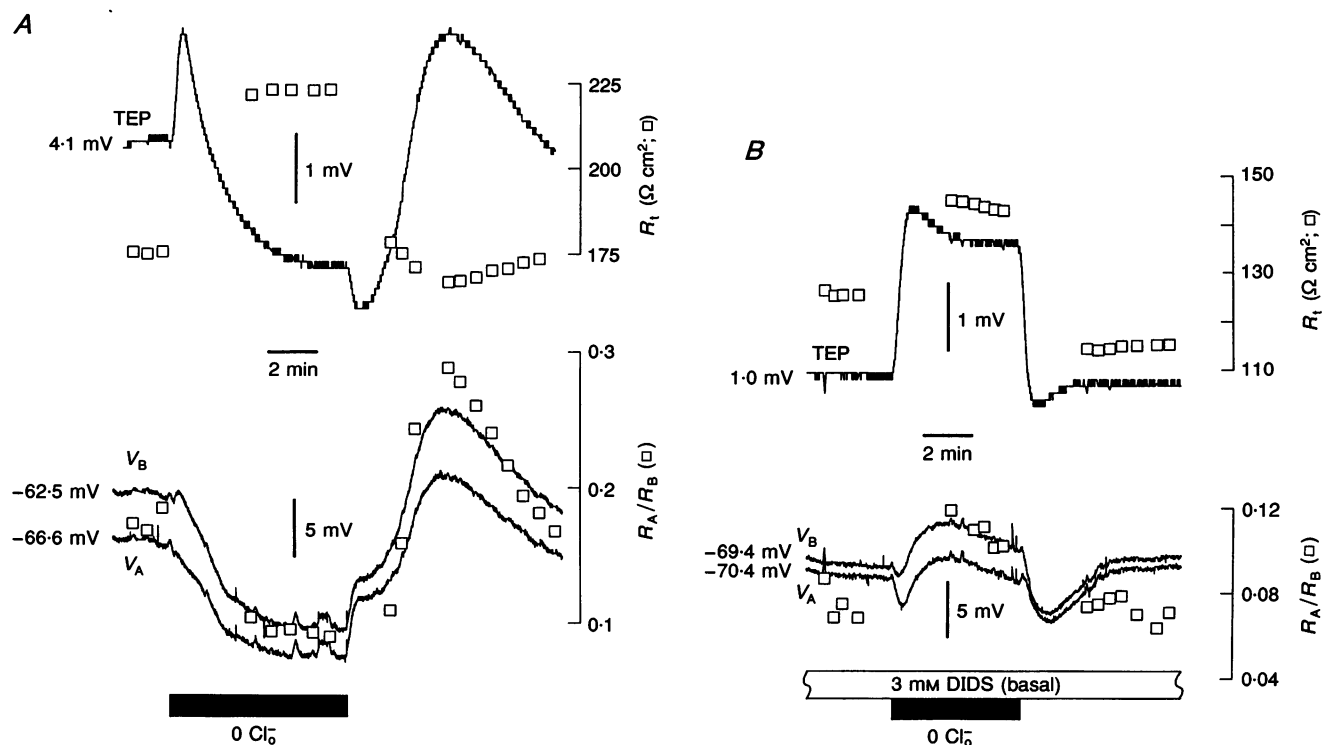


**Figure 5. Apical  $Cl^-$  removal produces a  $V_B$  hyperpolarization that is DIDS inhibitable**

*A*, the effect of apical  $Cl^-$  removal ( $CH_3SO_4$  replacement) on TEP and  $R_t$  (upper trace), and  $V_A$ ,  $V_B$  and  $a$  (lower trace). The initial transient TEP increase was due to a liquid junction potential in the apical bath. Both membranes hyperpolarized and there was a steady-state decrease in TEP in response to  $Cl^-$  removal;  $a$  decreased and  $R_t$  increased concomitantly with the membrane voltage changes. *B*, the effect of apical  $Cl^-$  removal on TEP and  $R_t$  (upper trace), and  $V_A$ ,  $V_B$  and  $a$  (lower trace) – all in the presence of basal DIDS (3 mM). The TEP increase was due to a liquid junction potential as in Fig. 5A. Basal DIDS inhibited the  $0\text{ Cl}_o^-$ -induced membrane hyperpolarizations and resistance changes.

$1.3 \pm 0.3$  mV, increased  $R_t$  by  $48 \pm 8 \Omega \text{ cm}^2$  and decreased  $a$  by  $0.14 \pm 0.4\%$  ( $n = 3$ ). Apical  $\text{Cl}^-$  removal also decreased  $a_{\text{Cl}^-}^i$  by  $26.3 \pm 4.7$  mM ( $n = 3$ , not shown).

Figure 5B shows that the hyperpolarization induced by the removal of apical  $\text{Cl}^-$  was blocked by 3 mM basal DIDS. The 0  $\text{Cl}^-$  response began with a TEP increase ( $V_A$  hyperpolarization) due to the liquid junction potential at the apical agar bridge (as in Fig. 5A). In the steady state, apical  $\text{Cl}^-$  removal depolarized  $V_B$  by 3.5 mV,  $R_t$  increased from 125 to 140  $\Omega \text{ cm}^2$  and  $a$  increased from 0.08 to 0.12. In a series of similar experiments, removing apical  $\text{Cl}^-$  in the presence of basal DIDS (3 mM) caused a small steady-state depolarization of  $V_B$  ( $1.9 \pm 1.3$  mV), which was not significantly different from zero.  $R_t$  increased by  $18 \pm 5 \Omega \text{ cm}^2$  and  $a$  increased by  $0.05 \pm 0.02$  ( $n = 3$ ). Thus, basal DIDS completely blocked the basolateral membrane voltage and resistance changes caused by apical  $\text{Cl}^-$  removal.

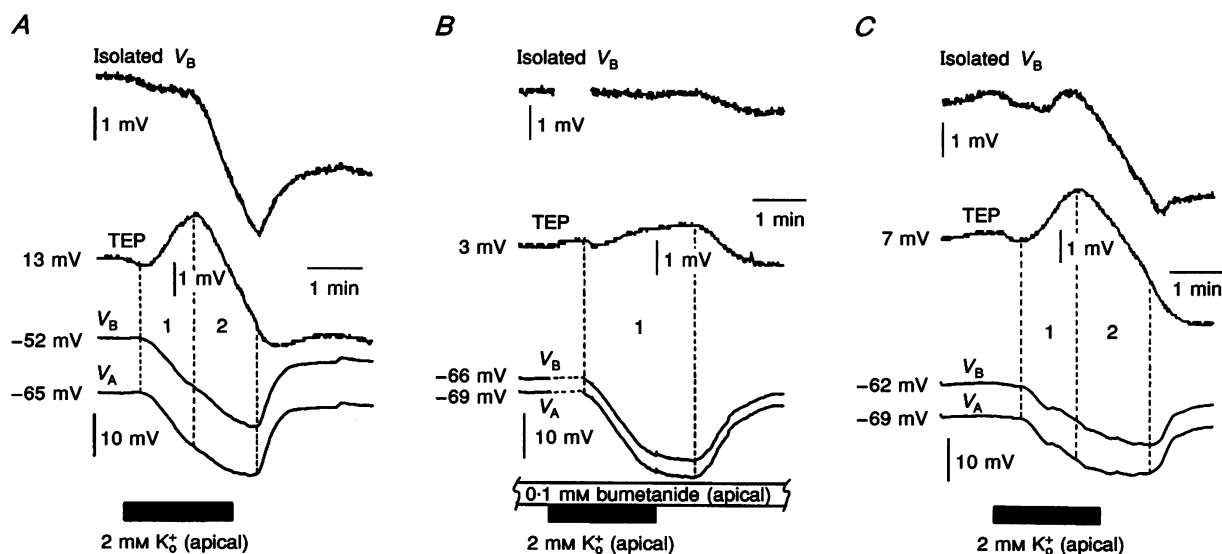
These results show that apical bumetanide (0.5 mM) and apical  $\text{Cl}^-$  removal both reduced  $a_{\text{Cl}^-}^i$  by 25–30 mM and had qualitatively similar effects on membrane voltage and resistance; they both hyperpolarized the basolateral membrane and decreased basolateral membrane conductance.

Figure 6 shows the effects of 0.1 mM apical bumetanide on the 5 to 2 mM  $\text{K}_o^+$  response. The isolated basolateral membrane response was calculated (Methods) and displayed in the upper trace of each panel. Figure 6A is a control response and shows that the isolated  $V_B$  hyper-

polarized by 4.2 mV during the DBMH. Figure 6B shows that 0.1 mM apical bumetanide eliminated the DBMH and completely blocked the isolated  $V_B$  hyperpolarization. Figure 6C is the following control after bumetanide was removed from the apical bath; the DBMH and the isolated  $V_B$  hyperpolarization were completely restored. These results were corroborated in a series of identical experiments ( $n = 6$ ) summarized in Table 1. They show that the  $\Delta[\text{K}^+]_o$ -induced delayed basolateral membrane hyperpolarization is mediated by the apical membrane, bumetanide-sensitive  $\text{Na}^+-\text{K}^+-2\text{Cl}^-$  cotransporter.

## DISCUSSION

The present experiments have analysed the membrane and cellular events that underlie the generation of the delayed basolateral membrane hyperpolarization in bovine RPE. Three disparate changes all produced qualitatively similar changes in cell  $\text{Cl}^-$  activity and in membrane voltage. Reducing apical  $[\text{K}^+]_o$ , or  $[\text{Cl}^-]_o$ , or adding bumetanide to the apical bath all decreased  $a_{\text{Cl}^-}^i$  and hyperpolarized both membranes. In each case a larger hyperpolarization was generated at the basolateral membrane, as evidenced by the decrease in TEP. These results and the observation that the delayed basolateral membrane hyperpolarization was practically abolished in the presence of bumetanide (Fig. 6, Table 1) strongly suggest that the apical membrane  $\text{Na}^+-\text{K}^+-2\text{Cl}^-$  cotransporter plays a crucial role in generating the 'delayed' basolateral membrane hyperpolarization (DBMH).



**Figure 6. Bumetanide eliminates phase 2 from the apical 5 to 2 mM  $\text{K}_o^+$  response**

The effect of reducing apical  $[\text{K}^+]_o$  from 5 to 2 mM in the absence and presence of apical bumetanide (0.1 mM). Isolated  $V_B$  (upper trace) was calculated as described in Methods. *A*, initial control, the step change in apical  $[\text{K}^+]_o$  resulted in a 5 mV hyperpolarization in the isolated  $V_B$  during phase 2. *B*, in the presence of bumetanide phase 2 was abolished and there was practically no isolated  $V_B$  response although both membranes hyperpolarized as expected. *C*, following control, phase 2 was completely recovered along with the isolated  $V_B$  hyperpolarization. The absence of phase 3 in all panels is probably due to the relatively short exposure of the apical membrane to 2 mM  $\text{K}_o^+$ .

In principle this conclusion could be more rigorously tested by first blocking the apical membrane  $K^+$  channels with  $Ba^{2+}$ , thereby circumventing phase 1 (Joseph & Miller, 1991). In this case one would expect to observe phase 2 in isolation. When apical  $[K^+]_o$  was changed from 5 to 2 mM in the presence of  $Ba^{2+}$ ,  $a_K^i$  and  $a_{Cl}^i$  decreased by only  $3 \pm 1$  and  $5 \pm 2$  mM, respectively ( $n = 3$ ). Phases 1 and 2 were both absent, and using these changes in  $a_K^i$  and  $a_{Cl}^i$ , the calculated  $E_B$  hyperpolarization was only 0.5 mV (eqn (5)). In the absence of  $Ba^{2+}$  the calculated  $E_B$  change is over eight times larger. Therefore, phase 2 is practically impossible to observe in the presence of apical  $Ba^{2+}$ .

These results can be understood if one considers the driving force on the apical membrane  $Na^+ - K^+ - 2Cl^-$  cotransporter in the presence and absence of  $Ba^{2+}$ . In the absence of  $Ba^{2+}$  the driving force on the cotransporter is 29 mV inward ( $a_K^i = 65$  mM,  $a_{Cl}^i = 65$  mM and  $a_{Na}^i = 5$  mM; Bialek & Miller, 1994; Kenyon *et al.* 1994). In the presence of apical  $Ba^{2+}$  the driving force is 12 mV inward. This calculation is based on the observation that  $Ba^{2+}$  increases  $a_{Cl}^i$  and  $a_K^i$  by  $18 \pm 7$  and  $9 \pm 5$  mM, respectively (Bialek & Miller, 1994); it assumes that  $a_{Na}^i$  remains unchanged. Therefore, if the cotransporter rate decreases with decreasing driving force, then the change in apical  $[K^+]_o$  should produce a significantly smaller DBMH in the presence of apical  $Ba^{2+}$ .

Our conclusion that the inward driving force of the cotransporter is reduced in the presence of  $Ba^{2+}$  was confirmed by measuring the bumetanide-induced membrane hyperpolarization, first in the absence then in the presence of apical  $Ba^{2+}$ . Apical  $Ba^{2+}$  significantly inhibited the bumetanide-induced voltage change ( $n = 2$ , not shown).

The DBMH was also abolished by basal DIDS (Table 1, column 4) indicating that the basolateral membrane  $Cl^-$  conductance is also an important determinant of this response. Since DIDS is covalently reactive, we considered the possibility that it could have non-specific effects on other channels or exchangers (Biagi, 1985; Inoue, 1985; Hughes, Adorante, Miller & Lin, 1989). For example, in bovine RPE the basolateral membrane is primarily conductive to  $Cl^-$  and  $K^+$ ;  $T_{Cl}^B \approx 0.6$  and  $T_K^B \approx 0.3$ . In the presence of DIDS,  $T_K^B \approx 0.99$  and therefore DIDS only blocked the basolateral membrane  $Cl^-$  conductance with no apparent effect on  $K^+$  conductance (Bialek & Miller, 1994). This conclusion was corroborated in tracer flux experiments which showed that  $^{36}Cl^-$  efflux across the basolateral membrane was completely blocked by DIDS (Miller & Edelman, 1990) and that DIDS had no effect on  $^{86}Rb^+$  ( $K^+$  substitute) flux across the basolateral membrane (Bialek & Miller, 1994).

#### DBMH: pH dependence

The  $\Delta[K^+]_o$ -induced decrease in  $a_{Cl}^i$  helps generate the DBMH and is accompanied by a decrease in  $pH_i$  (Kenyon *et al.* 1990). The two mechanisms that help generate the DBMH, the apical membrane  $Na^+ - K^+ - 2Cl^-$  cotransporter

and the basolateral membrane  $Cl^-$  channel, could have caused the  $pH_i$  decrease – perhaps indirectly via the decrease in  $a_{Cl}^i$ . This is an unlikely possibility because the apical addition of bumetanide, the removal of apical  $Cl^-$ , or the addition of DIDS to the basal bath had no significant effect on  $pH_i$  ( $n = 5$ , E. Kenyon & S. S. Miller, unpublished observations).

Conversely, one might imagine that the decrease in  $pH_i$  directly or indirectly altered  $a_{Cl}^i$  and therefore helped generate the DBMH. This could have occurred because the apical reduction of  $[K^+]_o$  from 5 to 2 mM ( $\Delta[K^+]_o$ ) decreased the inward driving force on the apical membrane electrogenic  $NaHCO_3$  cotransporter; the subsequent drop in  $[HCO_3^-]_i$  ( $pH_i$ ) could then have decreased the rate of the basolateral membrane  $Cl^- - HCO_3^-$  exchanger and decreased  $a_{Cl}^i$  as shown in frog RPE (Fong, Bialek, Hughes & Miller, 1988; Lin & Miller, 1991, 1994). Against this interpretation is the observation that  $HCO_3^-$  removal from both bathing solutions did not significantly alter the  $\Delta[K^+]_o$ -induced change in  $a_{Cl}^i$  or the DBMH (Fig. 3).

These data suggest that the  $\Delta[K^+]_o$ -induced changes in  $a_{Cl}^i$  and  $pH_i$  are produced by two separate transport pathways that do not strongly affect one another. This conclusion, however, does not eliminate the possibility that  $a_{Cl}^i$  (and the DBMH) was altered by  $\Delta[K^+]_o$ -induced changes in  $pH_i$ ; this could have occurred by mechanisms we have not yet identified. In order to estimate the theoretically maximum possible  $pH_i$ -induced change in  $a_{Cl}^i$ , we have measured the  $CO_2$ -induced changes in  $a_{Cl}^i$  and  $pH_i$ . These two linear relationships (Results) were combined to obtain the change in  $a_{Cl}^i$  (1.9 mM) per 0.1 pH unit. This ratio, multiplied by the  $\Delta[K^+]_o$ -induced change in  $pH_i$  provides a theoretical upper bound for the  $pH_i$ -induced change in  $a_{Cl}^i$ . Since the apical 5 to 2 mM  $[K^+]_o$  change acidified the cells by  $0.3 \pm 0.09$  pH units ( $n = 14$ ) (control  $pH_i \approx 7.4$ ) the maximum possible decrease in  $a_{Cl}^i$  was 5.7 mM. In comparison, the apical 5 to 2 mM  $K^+$  change decreased  $a_{Cl}^i$  by 25 mM, more than four times greater than the maximum effect of pH alone. Furthermore, during the DBMH,  $pH_i$  decreased by only  $0.15 \pm 0.03$ , which would result in an  $a_{Cl}^i$  decrease of 2.9 mM. The measured  $a_{Cl}^i$  decrease during the DBMH was 14 mM, almost five times greater than that predicted by pH alone. Therefore, the  $\Delta[K^+]_o$ -induced changes in  $pH_i$  are not a major determinant of the DBMH.

#### $Cl^-$ (and $K^+$ ) contributions to the DBMH

The  $a_{Cl}^i$  decrease that occurs during the DBMH could hyperpolarize  $V_B$  in at least two ways: (1) by altering the Nernst potential for  $Cl^-$  ( $E_{Cl}$ ); and (2) by decreasing the basolateral membrane  $Cl^-$  conductance ( $g_{Cl}^B$ ). In addition, we previously demonstrated that intracellular potassium ( $a_K^i$ ) also decreased during the DBMH with a magnitude and time course similar to the decrease in  $a_{Cl}^i$  (Bialek & Miller, 1994). Therefore, the  $\Delta[K^+]_o$ -induced changes in both  $a_{Cl}^i$  and  $a_K^i$  could contribute to the DBMH.

The apical  $\Delta[K^+]_o$ -induced changes in intracellular  $K^+$  and  $Cl^-$  along with the membrane voltage and resistance changes were used to construct a model that predicts the relative contributions of the  $a_{Cl}^i$  and  $a_K^i$  changes to the DBMH. The model uses calculated changes in  $E_{Cl}$  and  $g_{Cl}^B$ , as well as  $E_K$  and  $g_K^B$ , during phase 2 to predict how each of these parameters affects the DBMH. Figure 7 summarizes the  $E_{Cl}$ ,  $E_K$ ,  $T_{Cl}^B$  and  $T_K^B$  changes that were calculated from intracellular  $Cl^-$ - and  $K^+$ -selective microelectrode data during a typical apical 5 to 2 mM  $K_o^+$  response. The  $T_{Cl}^B$  and  $T_K^B$  values in Fig. 7 were obtained using eqns (6)–(8) at each point that resistance measurements were made (see below). Although the data came from two different tissues, the voltage responses for each tissue were nearly identical. All of these four factors potentially play a role in determining the magnitude and time course of the DBMH (phase 2); model calculations provide a way to assess their contributions to the DBMH.

**The model**

These calculations utilize the results of previous experiments (Joseph & Miller, 1991) which provide upper and lower bounds for the shunt resistance ( $R_s$ ). As shown in Fig. 1,  $R_t$  increased when apical  $[K^+]_o$  was decreased from 5 to 2 mM. Some of this increase occurred because the basolateral membrane resistance increased (see below), but more importantly we considered the possibility that part of the  $R_t$  increase was due to an increase in  $R_s$ . To help ensure that the conclusions of the model are

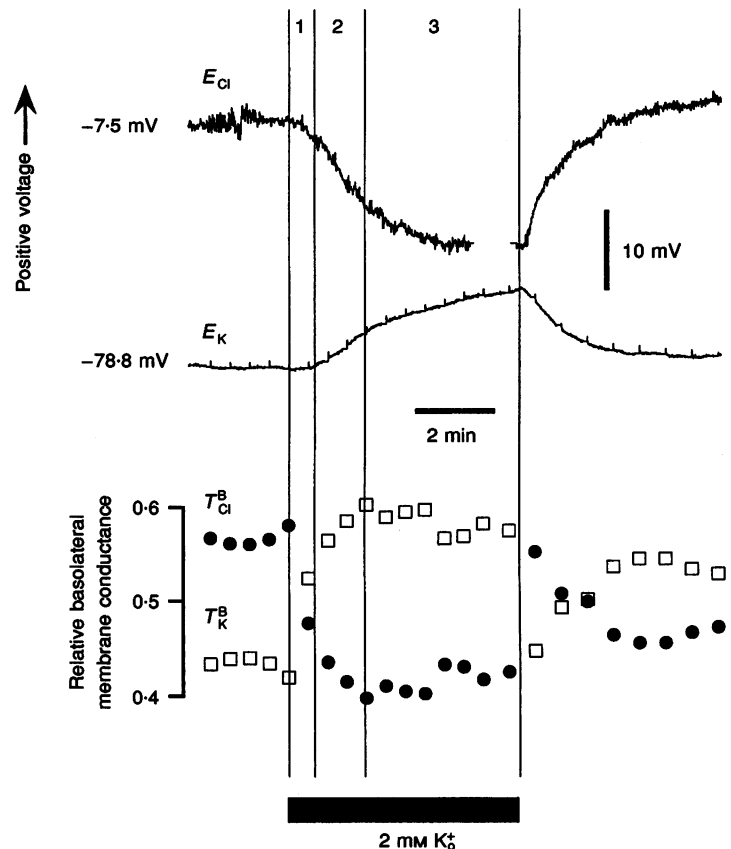
independent of the assumed value for  $R_s$ , we allowed the initial value of  $R_s$  (at the beginning of phase 2) to vary between  $1.10R_t$  and  $1.15R_t$ ; this range of uncertainty in  $R_s$  has been experimentally determined (Joseph & Miller, 1991). If  $R_s$  is assumed to remain constant, decrease, or undergo an increase larger than the percentage increase observed in  $R_t$  ( $8 \pm 2\%$ ,  $n = 6$ ) then the model gave physically impossible results (e.g. membrane conductances with negative values). Thus, only cases in which  $R_s$  increased by an amount less than the percentage change in  $R_t$  were considered.

The calculated values of  $E_B$ ,  $g_{Cl}$  and  $g_K$  (key elements of the model) are dependent on the assumed relationship between  $R_s$  and  $R_t$ . The initial value of  $R_s$  (at the start of phase 2) was varied from  $1.10R_t$  to  $1.15R_t$ ; the increase in  $R_s$  during phase 2 varied from 2 to 7%. Given these assumptions, the calculated  $E_B$  ranged from  $-18.2$  to  $-34.8$  mV at the start of phase 2 and from  $-36.2$  to  $-50.3$  mV at the end of phase 2. Similarly,  $g_{Cl}$  ranged from  $615$  to  $629 \mu S cm^{-2}$  at the start of phase 2 and from  $340$  to  $423 \mu S cm^{-2}$  at the end of phase 2;  $g_K$  ranged from  $128$  to  $329 \mu S cm^{-2}$  at the start of phase 2 and from  $243$  to  $430 \mu S cm^{-2}$  at the end of phase 2. The main conclusions of this analysis are unaffected by the choice of  $R_s$ .

As a specific example we assumed that  $R_s$  was  $1.14R_t$  at the beginning of phase 2 and increased by 5%. Given these assumptions and using eqn (7) along with the membrane voltage and resistance data from six tissues,  $E_B$  was calculated to be  $-35 \pm 4$  mV at the beginning of phase 2 and  $-45 \pm 4$  mV at the end of phase 2. Similarly,

**Figure 7.  $E_{Cl}$ ,  $E_K$ ,  $T_{Cl}^B$  and  $T_K^B$  during the apical 5 to 2 mM  $K_o^+$  response**

The intracellular  $K^+$  and  $Cl^-$  data were obtained from two different tissues, but in both tissues the voltage and resistance responses to the change in apical  $[K^+]_o$  were practically identical. The  $T_{Cl}^B$  and  $T_K^B$  values were obtained using eqns (6)–(8) at each point that resistance measurements were made (see text).



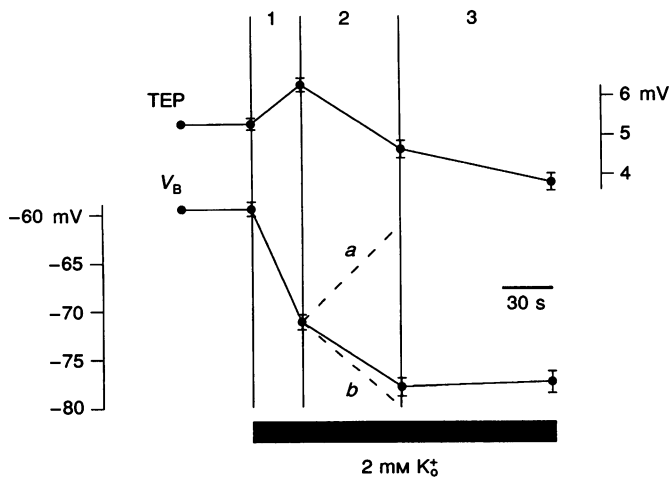


**Figure 8. Modelling the  $a_{Cl}^i$  and  $a_K^i$  contributions to the DBMH**

A model that considers the changes in  $a_{Cl}^i$  and  $a_K^i$  and their effects on the DBMH (phase 2), separately. The continuous lines are the normalized TEP and  $V_B$  responses measured at five points (filled circles) during the apical 5 to 2 mM  $K_o^+$  change ( $n = 6$  tissues). The initial points in the TEP and  $V_B$  traces are the mean starting values; errors bars represent the s.e.m. between the data points and the starting values for each tissue. Dashed lines represent theoretical phase 2 responses under the following assumptions: in *a*,  $E_{Cl}$  and  $g_{Cl}^B$  are held constant while  $E_K$  and  $g_K^B$  vary through their calculated values; in *b*,  $E_K$  and  $g_K^B$  are held constant while  $E_{Cl}$  and  $g_{Cl}^B$  vary.

the total basolateral membrane conductance,  $G_B$ , was  $940 \mu S cm^{-2}$  at the beginning of phase 2 and  $720 \mu S cm^{-2}$  at the end of phase 2 (eqn (8)). Using the intracellular  $Cl^-$  and  $K^+$  data from fifteen experiments (9 for  $Cl^-$  and 6 for  $K^+$ ),  $E_{Cl}$  and  $E_K$  were calculated to be  $-14 \pm 5$  and  $-74 \pm 3$  mV at the beginning of phase 2 and  $-23 \pm 6$  and  $-68 \pm 4$  mV at the end of phase 2, respectively. These values of  $E_{Cl}$  and  $E_K$  along with the calculated  $E_B$  indicate that  $T_{Cl}^B$  decreased by 0.13 during phase 2, from 0.65 to 0.52 (eqn (6)). Therefore, the basolateral membrane  $Cl^-$  conductance,  $g_{Cl}^B (= T_{Cl}^B \times G_B)$ , decreased by  $240 \mu S cm^{-2}$  during phase 2, from 610 to  $370 \mu S cm^{-2}$ . In contrast, the basolateral membrane  $K^+$  conductance,  $g_K^B$ , increased slightly during phase 2 from 330 to  $350 \mu S cm^{-2}$  (assuming  $g_K^B = G_B - g_{Cl}^B$ ).

The calculated decrease in  $g_{Cl}^B$  during phase 2, which occurred in each case, was expected given the observed decrease in  $a_{Cl}^i$ ; however, the calculated  $g_K^B$  increase was surprising because  $a_K^i$  decreased (Bialek & Miller, 1994). One possibility is that the  $\Delta[K^+]_o$ -induced hyperpolarization of  $V_B$  increased the basolateral membrane  $K^+$  conductance. Inward rectification of this type has been observed in bullfrog RPE (Hughes & Segawa, 1993). In the present model, the calculated  $g_K^B$  sometimes decreased depending on the assumptions made about  $R_B$ , but in every case the change in  $g_K^B$  was associated with a basolateral membrane depolarization during phase 2.

Figure 8 shows the results of the model calculation for the DBMH. The continuous traces of TEP and  $V_B$  are the mean measured values at five points (filled circles) during the apical 5 to 2 mM  $K_o^+$  responses ( $n = 6$ ). In trace *a* (dashed line)  $E_{Cl}$  and  $g_{Cl}^B$  were assumed to remain constant during phase 2 (DBMH). The change in  $V_B$  during the DBMH was then calculated using only the changes in  $a_K^i$ . Conversely, in trace *b*,  $E_K$  and  $g_K^B$  were assumed constant and only the changes in  $a_{Cl}^i$  were used to calculate the changes in  $V_B$  during the DBMH. In this case the phase 2 hyperpolarization closely approximated the observed phase 2 response (continuous line). This analysis indicates that the DBMH is mainly due to the  $\Delta a_{Cl}^i$ -induced changes in  $E_{Cl}$  and  $g_{Cl}$ .

#### DBMH: role of the $Na^+ - K^+ - 2Cl^-$ cotransporter

The  $\Delta[K^+]_o$ -induced decrease in  $a_{Cl}^i$  could have occurred because of a decrease in net  $Cl^-$  influx across the apical membrane or because of an increase in net  $Cl^-$  efflux across the basolateral membrane. Since conductive ion flux is the product of electrochemical driving force and membrane conductance, both factors must be considered. In Fig. 9 the electrochemical driving force for  $Cl^-$  exit across the basolateral membrane ( $V_B - E_{Cl}$ ) was calculated using the data in Fig. 1; an upward deflection on the trace in Fig. 9 signifies an increased outward driving force.

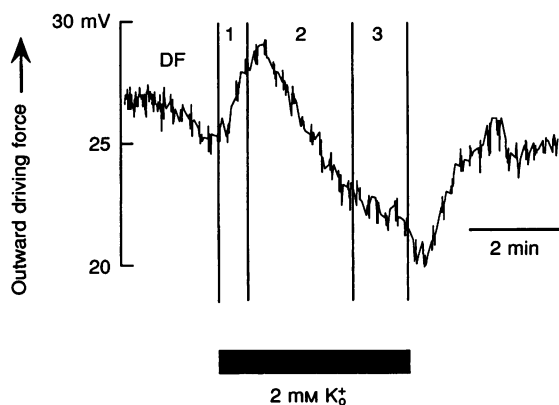


**Figure 9. The driving force for  $Cl^-$  exit during the apical 5 to 2 mM  $K_o^+$  response**

The electrochemical driving force (DF) for  $Cl^-$  exit across the basolateral membrane during the apical 5 to 2 mM  $K_o^+$  change from Fig. 1. An upward deflection represents an increasing outward driving force (mV). During phase 1 the driving force for  $Cl^-$  exit across the basolateral membrane increased, but during phases 2 and 3 the outward driving force decreased. DF is calculated from the difference between  $E_{Cl}$  (the Nernst potential for  $Cl^-$ ) and  $V_B$  (the measured basolateral membrane potential).

During phase 1 the driving force for  $\text{Cl}^-$  exit increased because  $V_B$  hyperpolarized at a greater rate than  $E_{\text{Cl}}$ . During most of phase 2 the opposite was true and the driving force for  $\text{Cl}^-$  exit decreased.

Figure 1 shows that the  $\Delta[\text{K}^+]_o$ -induced decrease in  $a_{\text{Cl}}^i$  is accompanied by an increase in  $R_t$  and a decrease in  $a$ . These resistance changes, consistent with a decrease in basolateral membrane conductance, provide part of the basis for the model calculations in Fig. 8 and the second section in small text (above). The data summarized in Fig. 1 was corroborated in a different series of experiments that also decreased  $a_{\text{Cl}}^i$ . Figures 4A and 5A show that apical bumetanide or the removal of apical  $\text{Cl}_o^-$  significantly decreased  $a_{\text{Cl}}^i$ , increased  $R_t$  and decreased  $a$  – consistent with a basolateral membrane conductance decrease. Figures 4B and 5B show that basal DIDS blocked the voltage and resistance changes produced by apical bumetanide or by apical  $\text{Cl}_o^-$  removal. Since basal DIDS also blocked  $^{36}\text{Cl}^-$  efflux from the basolateral membrane (Miller & Edelman, 1990), it seems most likely that the bumetanide and 0  $\text{Cl}_o^-$ -induced changes in basolateral membrane resistance are mediated by a  $\text{Cl}^-$  conductive mechanism, presumably a  $\text{Cl}^-$  channel. Because DIDS blocks basolateral membrane  $\text{Cl}^-$  conductance and significantly inhibited the  $\Delta[\text{K}^+]_o$ -induced changes in cell  $\text{Cl}^-$ ,  $R_t$  and  $a$  (Bialek & Miller, 1994), we conclude that  $g_{\text{Cl}}^B$  decreased during the DBMH (phase 2).

During phase 2 both the driving force for  $\text{Cl}^-$  exit across the basolateral membrane and the basolateral membrane conductance decreased. Therefore, the decrease in cell  $\text{Cl}^-$  during the DBMH can only be accounted for by a decrease in  $\text{Cl}^-$  entry at the apical membrane. This entry mechanism is almost certainly the  $\text{Na}^+-\text{K}^+-2\text{Cl}^-$  cotransporter since apical bumetanide blocked the DBMH (Fig. 6 and Table 1). The decrease in  $\text{Cl}^-$  entry that generated the DBMH during phase 2 was caused by a  $\Delta[\text{K}^+]_o$ -induced decrease in driving force on the cotransporter (Bialek & Miller, 1994) and possibly by a kinetic reduction in cotransport rate.

### RPE physiology

The present results demonstrate that both components of the  $\text{Cl}^-$  transport pathway are necessary for observing the DBMH. In the intact eye this voltage response is initiated by a light-induced decrease of  $[\text{K}^+]_o$  in the extracellular (or subretinal) space that separates the photoreceptors and the RPE apical membrane (Griff & Steinberg, 1984; Linsenmeier & Steinberg, 1984). *In vitro*, the effects of light can be approximated by a step decrease in apical  $[\text{K}^+]_o$  (Fig. 1; Steinberg *et al.* 1985).

To what extent can the present analysis be extended to the human eye? Intra- and extracellular electrical recordings from intact cat and monkey eyes (Valeton & van Norren, 1982; Steinberg *et al.* 1985) and from other *in*

*vitro* preparations (Gallemore & Steinberg, 1993) have been used to determine the membrane voltage and resistance responses that underlie two clinically diagnostic signals. These signals, the 'fast oscillation' (FO) and the 'light peak' (LP) are obtained by using extracellular electrodes placed across the human eye. They are recorded as a part of the electro-oculogram (EOG) or as a part of the DC-electroretinogram (ERG) (Marmor & Lurie, 1979; Weleber, 1989). The FO occurs ~20 s after light onset and is generated by a basolateral membrane hyperpolarization (DBMH). The LP occurs ~5 min after light onset and is generated by a depolarization of the basolateral membrane (Griff & Steinberg, 1982; Linsenmeier & Steinberg 1982; Steinberg *et al.* 1985). In both cases, the data from animal experiments provide good evidence to suggest that the FO and LP are generated, in the human eye, at the basolateral membrane  $\text{Cl}^-$  channels (Gallemore & Steinberg, 1993).

The present *in vitro* results in bovine RPE, coupled with a similar but less complete analysis in native fetal human RPE (Quinn & Miller, 1992; R. H. Quinn & S. S. Miller, unpublished observations), strongly supports that conclusion. As a further test we have carried out a series of FO and LP measurements (using the EOG) on normal individuals and on patients with cystic fibrosis (CF). CF is a genetic disease that commonly occurs in epithelia and results in the functional loss of plasma membrane cyclic AMP-dependent  $\text{Cl}^-$  channels (Cheng *et al.* 1993). RPE from adult human donor eyes also express the messenger RNA for this protein (Miller *et al.* 1992). We found that the FO signal was significantly reduced in CF patients compared with normal individuals. In contrast, the LP signal was normal. This result indicates that the FO is generated by a cyclic AMP-dependent  $\text{Cl}^-$  channel and that the LP is generated by a separate protein, perhaps the  $\text{Ca}^{2+}$ -dependent  $\text{Cl}^-$  channel, which is functionally normal in other CF epithelia (Anderson & Welsh, 1991; Stutts, Chinnet, Mason, Fullton, Clarke & Boucher, 1992; Jiang, Finkbeiner, Widdicombe, McCray & Miller, 1993).

It will be useful to learn if the apical membrane  $\text{Na}^+-\text{K}^+-2\text{Cl}^-$  cotransporter or basolateral membrane  $\text{Cl}^-$  channel(s) are the source or endpoint of retinal/RPE diseases in patients with abnormal fast oscillations or light peaks (Weleber, 1989).

ANDERSON, M. P. & WELSH, M. J. (1991). Calcium and cAMP activate different chloride channels in the apical membrane of normal and cystic fibrosis epithelia. *Proceedings of the National Academy of Sciences of the USA* 88, 6003–6007.

BIAGI, B. A. (1985). Effects of the anion transport inhibitor, SITS, on the proximal straight tubule of the rabbit perfused *in vitro*. *Journal of Membrane Biology* 88, 25–31.

- BIALEK, S. & MILLER, S. S. (1994).  $K^+$  and  $Cl^-$  transport mechanisms in bovine pigment epithelium that could modulate subretinal space volume and composition. *Journal of Physiology* **475**, 401–417.
- CHENG, S. H., GREGORY, R. J., AMARA, J. F., RICH, D. P., ANDERSON, M., WELSH, M. J. & SMITH, A. E. (1993). Defective intracellular processing of CFTR as the molecular basis of cystic fibrosis. In *Cystic Fibrosis – Current Topics*, vol. 1, ed. DODGE, J. A., BROCK, D. J. H. & WIDDICOMBE, J. H., pp. 175–189. John Wiley & Sons, New York.
- DEARRY, A. & BURNSIDE, B. (1989). Light-induced dopamine release from teleost retinas acts as a light-adaptive signal to the retinal pigment epithelium. *Journal of Neurochemistry* **53**, 870–878.
- EDELMAN, J. L. & MILLER, S. S. (1991). Epinephrine stimulates fluid absorption across bovine retinal pigment epithelium. *Investigative Ophthalmology and Visual Science* **32**, 3033–3040.
- FONG, C. N., BIALEK, S., HUGHES, B. A. & MILLER, S. S. (1988). Modulation of intracellular chloride in bullfrog retinal pigment epithelium (RPE). *Federation Proceedings* **2**, A1722.
- GALLEMORE, R. P. & STEINBERG, R. H. (1993). Light-evoked modulation of basolateral membrane  $Cl^-$  conductance in chick retinal pigment epithelium: the light peak and fast oscillation. *Journal of Neurophysiology* **70**, 1669–1680.
- GALLEMORE, R. P., YAMAMOTO, F. & STEINBERG, R. H. (1990).  $[Ca^{2+}]_o$  gradients and light-evoked  $[Ca^{2+}]_o$  changes in cat retina, *in vivo*. *Society for Neuroscience Abstracts* **16**, 714.
- GARCIA, D. M. & BURNSIDE, B. (1994). Suppression of cAMP-induced pigment granule aggregation in RPE by organic anion transport inhibitors. *Investigative Ophthalmology and Visual Science* **35**, 178–188.
- GARCIA-DIAZ, J. F., STUMP, S. & ARMSTRONG, W. M. (1984). Electronic devices for microelectrode recordings in epithelial cells. *American Journal of Physiology* **246**, C339–346.
- GRIFF, E. R. (1991). Potassium-evoked responses from the retinal pigment epithelium of the toad *Bufo marinus*. *Experimental Eye Research* **53**, 219–228.
- GRIFF, E. R. & STEINBERG, R. H. (1982). Origin of the light peak: *in vitro* study of *Gekko gekko*. *Journal of Physiology* **331**, 637–652.
- GRIFF, E. R. & STEINBERG, R. H. (1984). Changes in apical  $[K^+]_i$  produce delayed basal membrane responses of the retinal pigment epithelium in the gecko. *Journal of General Physiology* **83**, 193–211.
- HUGHES, B. A., ADORANTE, J. S., MILLER, S. S. & LIN, H. (1989). Apical electrogenic  $NaHCO_3$  cotransport: a mechanism for  $HCO_3^-$  absorption across the retinal pigment epithelium. *Journal of General Physiology* **94**, 125–150.
- INOUE, I. (1985). Voltage-dependent chloride conductance of squid axon membrane and its blockade by some disulfonic stilbene derivatives. *Journal of General Physiology* **85**, 519–537.
- JIANG, C., FINKBEINER, W. E., WIDDICOMBE, J. H., MCCRAY, P. B. JR & MILLER, S. S. (1993). Altered fluid transport across airway epithelium in cystic fibrosis. *Science* **262**, 424–427.
- JOSEPH, D. P. & MILLER, S. S. (1991). Apical and basal membrane ion transport mechanisms in bovine retinal pigment epithelium. *Journal of Physiology* **435**, 439–463.
- JOSEPH, D. P. & MILLER, S. S. (1992). Alpha-1 adrenergic modulation of K and Cl transport in bovine retinal pigment epithelium. *Journal of General Physiology* **99**, 263–290.
- KENYON, E., MILLER, S. S. & ADORANTE, J. S. (1990). Apical  $[K]_o$  modulates  $pH_i$  in bovine RPE. *Investigative Ophthalmology and Visual Science* **31**, 70.
- KENYON, E., YU, K., LA COUR, M. & MILLER, S. S. (1994). Lactate transport mechanisms at the apical and basolateral membranes of bovine retinal pigment epithelium. *American Journal of Physiology* **267**, C1561–1573.
- LIN, H. & MILLER, S. S. (1991).  $pH_i$  regulation in frog retinal pigment epithelium: two apical membrane mechanisms. *American Journal of Physiology* **261**, C132–142.
- LIN, H. & MILLER, S. S. (1994).  $pH_i$ -dependent  $Cl^-HCO_3^-$  exchange at the basolateral membrane of frog retinal pigment epithelium. *American Journal of Physiology* **266**, C935–966.
- LINSENMEIER, R. A. & STEINBERG, R. H. (1982). Origin and sensitivity of the light peak of the intact cat eye. *Journal of Physiology* **331**, 653–673.
- LINSENMEIER, R. A. & STEINBERG, R. H. (1984). Delayed basal hyperpolarization of cat retinal pigment epithelium and its relation to the fast oscillation of the DC electroretinogram. *Journal of General Physiology* **83**, 213–232.
- MARMOR, M. F. & LURIE, M. (1979). Light-induced electrical responses of the retinal pigment epithelium. In *The Retinal Pigment Epithelium*, ed. ZINN, K. & MARMOR, M., pp. 226–244. Harvard University Press, Cambridge, MA, USA.
- MILLER, S. S. & EDELMAN, J. L. (1990). Active ion transport pathways in the bovine retinal pigment epithelium. *Journal of Physiology* **424**, 283–300.
- MILLER, S. S., RABIN, J., STRONG, T., IANNUZZI, M., ADAMS, A., COLLINS, F., REENSTRA, W. & MCCRAY, P. JR (1992). Cystic fibrosis (CF) gene product is expressed in retina and retinal pigment epithelium. *Investigative Ophthalmology and Visual Science* **33**, 1009.
- MILLER, S. S. & STEINBERG, R. H. (1977). Passive ionic properties of frog retinal pigment epithelium. *Journal of Membrane Biology* **36**, 337–372.
- NEWMAN, E. A. (1985). Membrane physiology of retinal glial (Müller) cells. *Journal of Neuroscience* **5**, 2225–2239.
- OAKLEY, B. II, MILLER, S. S. & STEINBERG, R. H. (1978). Effects of intracellular potassium upon the electrogenic pump of frog retinal pigment epithelium. *Journal of Membrane Biology* **44**, 281–307.
- QUINN, R. H. & MILLER, S. S. (1992). Ion transport mechanisms in native human retinal pigment epithelium. *Investigative Ophthalmology and Visual Science* **33**, 3513–3527.
- RINK, T. J., TSIEN, R. Y. & POZZAN, T. (1982). Cytoplasmic pH and free  $Mg^{2+}$  in lymphocytes. *Journal of Cell Biology* **96**, 189–196.
- SHIMAZAKI, H. & OAKLEY, B. II (1984). Reaccumulation of  $[K^+]_o$  in the toad retina during maintained illumination. *Journal of General Physiology* **84**, 475–504.
- STEINBERG, R. H., LINSSENMEIER, R. A. & GRIFF, E. R. (1985). Retinal pigment epithelial cell contributions to the electroretinogram and electrooculogram. In *Progress in Retinal Research*, vol. 4, ed. OSBORNE, N. N. & CHADER, G. J., pp. 33–66. Pergamon Press, Oxford, New York.
- STEINBERG, R. H., SCHMIDT, R. & BROWN, K. T. (1970). Intracellular responses to light from cat pigment epithelium: origin of the electroretinogram c-wave. *Nature* **227**, 728–730.
- STUTTS, M. J., CHINET, T. C., MASON, S. J., FULLTON, J. M., CLARKE, L. L. & BOUCHER, R. C. (1992). Regulation of Cl channels in normal and cystic fibrosis airway epithelial cells by extracellular ATP. *Proceedings of the National Academy of Sciences of the USA* **89**, 1621–1625.
- VALETON, J. M. & VAN NORREN, D. (1982). Intraretinal recordings of slow electrical responses to steady illumination in monkey: isolation of receptor responses and the origin of the light peak. *Vision Research* **22**, 393–399.

- WEAST, R. C. (1978). *CRC Handbook of Chemistry and Physics*, ed. WEAST, R. C., p. D-153. CRC Press, Inc, Cleveland, OH, USA.
- WELEBER, R. G. (1989). Fast and slow oscillations of the electro-oculogram in Best's macular dystrophy and retinitis pigmentosa. *Archives of Ophthalmology* 107, 530–537.
- YAMAMOTO, F., BORGULA, G. A. & STEINBERG, R. H. (1992). Effects of light and darkness on pH outside rod photoreceptors in the cat retina. *Experimental Eye Research* 54, 685–697.

#### **Acknowledgements**

It is our pleasure to thank Emily Kenyon for providing the intracellular pH measurements. The work was supported by NIH grant EY-02205 and Core grant EY-03176.

*Received 3 March 1994; accepted 13 September 1994.*